Mohamed E. El-Shimy [1,*], **S.A. Zaid** [2]

J. Electrical Systems 12-4 (2016): 687-700

Regular paper

Journal of Electrical Systems

Fuzzy PID Controller for Fast Direct Torque Control of Induction Motor Drives

Direct torque control (DTC) has been employed to give fast torque response, which is very important in traction and electric vehicle applications, in high dynamic performance Induction Motor (IM) drives. Fast torque response can be achieved by optimizing the selection of the inverter voltage vectors in the conventional DTC. This paper introduces a method for selecting voltage vectors; in DTC controlled IM drives, to achieve fast torque response at constant switching frequency. Also, the application of the Fuzzy PID (FPID) control technique improves the system speed and torque responses. Simulation results show that both torque and speed responses are faster with the proposed controller than the conventional DTC.

Keywords: Direct torque control (DTC); Fuzzy PID controller (FPID); Induction Motor (IM); conventional PID controller.

Article history: Received 22 July 2016, Accepted 15 October 2016

1. Introduction

High performance IM Drives are used in machine tools, spindles, high speed elevators, dynamometers, mine winders, rolling mills, electric vehicle, glass flat lines, and the like that have much more sophisticated requirements. Such high performance applications typically require high speed holding accuracy better than 0.5%, wide range speed control of at least 20:1 and fast transient response, typically better than 50 rad/s for the speed loop [1-4]. Achieving high performance drive, fast transient and accurate torque control is the key.

The fastest, simple, and accurate torque control technique for IM drives is the DTC [5]. Besides high torque dynamics, it is well known for being robust to the motor parameters change, except the stator resistance [5, 6]. It was introduced by [6] and [7] (Direct self control). Although it is simple and gives large benefits, the main drawback of it was the wide band of the switching frequency of the inverter even when the flux and torque references are kept constant [8]. This is due to the nature of the hysteresis controllers used for the torque and flux. The second step in the development of the DTC concept was introducing constant sampling techniques which replace the conventional analogue hysteresis controllers. Hence, the inverter upper switching frequency is limited. In case of constant sampling frequency, several authors have proposed various additions and variations of the DTC concept [9-15]. However, the majority of them do not guarantee the fastest torque response [16, 17].

Recently some attempts to promote the torque response of the DTC of the IM drives. References [16, 17], apply the dynamic over modulation technique to the optimization proposed by [8] to give fast torque response. It rely decrease the response time, but on the expense of the bad flux response and increased harmonic content due to the over modulation technique used.

[*] Corresponding author: Mohamed Ewis El-Shimy, Department of Electrical Engineering, Faculty of Engineering, University of Tabuk, Tabuk, Saudi Arabia, 741 Tabuk 71491, E-mail: mshimy2006@yahoo.co.in

[1] Department of Electrical Engineering, Faculty of Engineering, University of Tabuk, Tabuk, Saudi Arabia.

[2] Department of Electrical Power and Machines, Faculty of Engineering, Cairo University, Egypt

Reference [18], introduces a DTC technique for an open end IM to give full load torque control with fast transient response to very low speeds of operation, with reduced switching frequency variation. However, the power system is complex and bulky, two inverters with two isolation power transformers. The control technique depends on IM steady state model and the fundamental component of the stator voltage vector which in turn, to the author opinion, makes the system apart from fast response.

Reference [19-23]; apply the model predictive control technique to the DTC concept of the IM drives. The average switching frequency and consequently the switching losses of the inverter are reduced. However, there is no advancement in the dynamic torque response and the online calculations are so large. Also the accuracy of the system is sensitive to the quality of the predictive controller and the motor parameters dependence in this scheme is larger than the basic DTC.

It is well known that, voltage vectors selections have the great effect on the IM drive torque response, in turn the speed and position responses too. Voltage vectors selections can be optimized to give fast torque response of the drive [8].

Normally, IM drive contains speed controllers to regulate the dive speed. Traditionally, the conventional controller used to control the speed of IM drive was PID [24]. This controller is simple, stable, easy to tune, and highly reliable. However, the use of conventional PID controller causes sometimes many problems like high overshoot, oscillation of speed and torque due to sudden changes in load and external disturbances [25, 26]. This behavior of the controller leads to deterioration of drive performance. So, to get rid of these disadvantages, an intelligent controller based on fuzzy logic is employed [27-35].

In this paper, an optimization method, that modifies the variable frequency DTC to be constant sampling DTC and make optimization for fast torque response, is introduced. Also, the FPI control technique is applied to improve the system speed and torque responses.

The voltage vectors optimization relations are derived, and then the system is Matlab simulated. The system response is analyzed and compared to the conventional DTC method. Also, FPI controller response is compared to the conventional PI controller.

2. Notation

The notation used throughout the paper is stated below.

Indexes:

V	the inverter DC voltage
θ	angle of the voltage vector
k	order of the voltage vector
λ_r	rotor flux vector
λ_s	stator flux vector
ω	angular velocity of the rotor flux
λ_o	initial value of the stator flux vector
θ_{ro}	rotor flux vector angle
T	motor torque
$\Delta\lambda$	flux error

ΔT torque error
e Speed error
Δe derivative of the speed error
T_{ref} reference torque
DTC Direct torque control
FPID Fuzzy PID controller
PID Proportional, Integral and Derivative
u Controller signal
ω_{ref} reference speed
τ Sampling time
e_n Normalized speed error
α proportional constant for integral gain

Constants:

K_p Proportional gain
K_i Integral gain
K_d Derivative gain
C Constant
K_{pp} Multiplication factor for proportional gain
K_{dd} Multiplication factor for derivative gain

3. Optimization of the voltage vectors selections for maximum torque rate

In the conventional DTC, hysteresis controllers control both the stator flux and the motor torque to be within a hysteresis band, as shown in Figure 1. Owing to the nature of the hysteresis controllers, there is no optimization in selecting the voltage vectors inside the flux hysteresis band. For example, as shown in Fig. 1, if the flux vector is at point 2 and the toque is to be increased, the hysteresis controller will select the same voltage vector as at point 1(i.e. if the previous selected voltage vector was $\boldsymbol{V}_4$, then the controller will select $\boldsymbol{V}_4$ also).

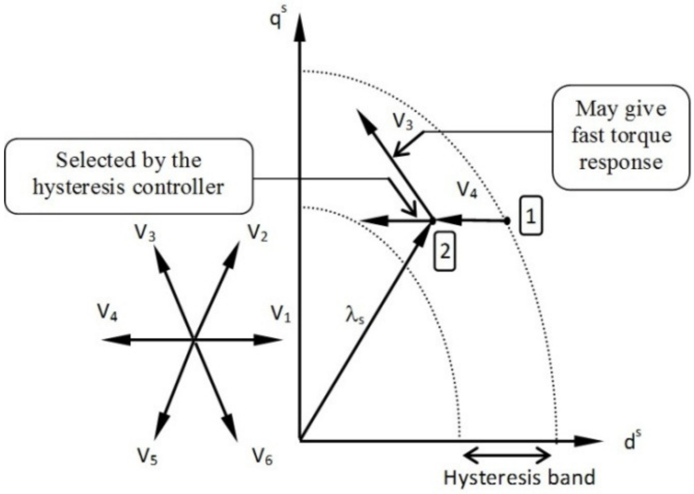

Figure 1: The possible stator flux vector trajectories inside the hysteresis band with DTC.

However, this selection may not give fast torque response. To achieve fast torque response the selection of the voltage vector, inside the hysteresis band, is optimized to give maximum rate of torque increase. The optimization process is as follows:

1. Derivation of the torque rate equation in terms of the applied voltage vector.

2. Comparison between the two possible voltage vectors according to the equation derived in step1.

The optimization process can be achieved as follows:
Consider the stator and rotor flux vectors of the IM, as shown in Figure 2, and assuming that the selected inverter voltage vector, Figure 1, is

$$\mathbf{V}_k = V\angle\theta_k$$

Where (V) is the inverter DC voltage, (θ_k) is the angle of the voltage vector, and (k) is the order of the voltage vector.

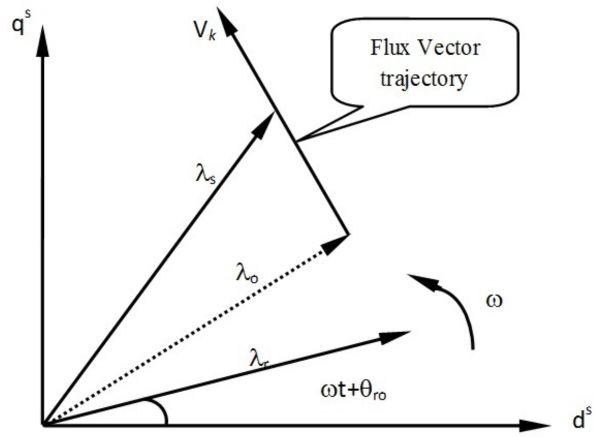

Figure 2: The stator and rotor flux vectors.

The rotor flux vector is assumed to rotate with a stable angular speed and amplitude during the operating period of the stator voltage vector [4]. The rotor flux vector can be written as:

$$\bar{\boldsymbol{\lambda}}_r = \lambda_r e^{j(\omega t+\theta_{ro})} \quad (1)$$

Where (ω) is the angular velocity of the rotor flux. Also assume that the initial value of the stator flux vector ($\bar{\boldsymbol{\lambda}}_o$), at the beginning of applying the voltage vector, is

$$\bar{\boldsymbol{\lambda}}_s\Big|_{t=0} = \bar{\boldsymbol{\lambda}}_o = \lambda_o\angle\theta_o \quad (2)$$

The basic equation of the stator flux vector in terms of the stator voltage vector can be derived as follows: neglecting the stator resistance we have

$$\mathbf{V}_k = \frac{d\bar{\boldsymbol{\lambda}}_s}{dt} \quad (3)$$

Then by integration we obtain the instantaneous stator flux vector

$$\bar{\boldsymbol{\lambda}}_s = \mathbf{V}_k t + \bar{\lambda}_o \quad (4)$$

Then the stator flux vector trajectory will move parallel to the voltage vector selected, as shown in Fig. 1. The motor torque is given by

$$T = C\,\mathrm{Im}\{\bar{\boldsymbol{\lambda}}_s \bar{\boldsymbol{\lambda}}_r^*\} \quad (5)$$

Where C is a constant, and then differentiate w.r.t. time

$$T = C\,\mathrm{Im}\{\frac{d\bar{\boldsymbol{\lambda}}_s}{dt}\bar{\boldsymbol{\lambda}}_r^* + \bar{\boldsymbol{\lambda}}_s\frac{d\bar{\boldsymbol{\lambda}}_r^*}{dt}\} \quad (6)$$

But from Equations (1) and (2)

$$\begin{cases} \dfrac{d\bar{\boldsymbol{\lambda}}_r^*}{dt} = -j\omega\bar{\boldsymbol{\lambda}}_r^* \\ \dfrac{d\bar{\boldsymbol{\lambda}}_s}{dt} = \mathbf{V}_k \end{cases} \tag{7}$$

Therefore substituting Equation (7) into (6)

$$T = C\,\mathrm{Im}\{\mathbf{V}_k\bar{\boldsymbol{\lambda}}_r^* + \bar{\boldsymbol{\lambda}}_s(-j\omega\bar{\boldsymbol{\lambda}}_r^*)\} \tag{8}$$

Substituting (4) into (8)

$$T = C\,\mathrm{Im}\{(\mathbf{V}_k - j\omega(\mathbf{V}_k t + \bar{\boldsymbol{\lambda}}_o))\bar{\boldsymbol{\lambda}}_r^*\} \tag{9}$$

Let $t = 0$ (the instant of applying the voltage vector), then take the imaginary part:

$$\frac{dT}{dt} = C\lambda_r\left[V\sin(\theta_k - \theta_{ro}) - \omega\lambda_o\cos(\theta_k - \theta_{ro})\right] \tag{10}$$

Note that the second term in the above equation is independent of the selected voltage vector. Then to compare between two different voltage vectors we can use the following reduced relation

$$\left[\frac{dT}{dt}\right]^{\backslash} = \sin(\theta_k - \theta_{ro}) \tag{11}$$

This leads to the following maximization problem

$$\mathrm{fn} = \max_k\left[\sin(\theta_k - \theta_{ro})\right] \tag{12}$$

The index k that maximizes function fn, determines the selected voltage vector V_k. Equation (11) cannot be calculated off line as it depends on the rotor position; also the sine angle cannot be used for comparison. The problem in using this equation is the computation of the rotor angle θ_{ro}. Hence, an observer for the rotor flux angle must be used. The rotor flux observer will use more motor parameters, especially the rotor time constant. The effect of parameters variations on the optimization process will be discussed in a subsequent paragraph.

4. Control algorithm

Figure 3 shows a block diagram for the proposed control system. The control algorithm is performed using constant sampling time. There are two control loops.

In the outer control loop, also called the speed control loop, the feedback speed signal is compared to the reference or set point speed generating the speed error. Then, the speed error is fed to the speed controller, which is a FPI controller and will be designed in the next paragraph.

In the inner loop, also called the torque optimization loop, the controller measures the phase currents then estimates the stator flux vector ($\bar{\boldsymbol{\lambda}}_s$), the motor torque ($T$) and the rotor flux vector angle (θ_{ro}). If the torque error is greater or equal to zero ($\Delta T \geq 0$), the controller selects a zero voltage vector. However, if the torque error is less than zero, then it selects an active voltage vector according to the flux error ($\Delta\lambda$).

If it is out of the specified hysteresis band, the controller gives the same voltage vector as the conventional DTC. However, if the flux error is inside the band, then an optimization process is carried out, according to Equation (12), to select the vector that gives maximum torque rate. The speed controller is FPI and will be discussed in the next paragraph.

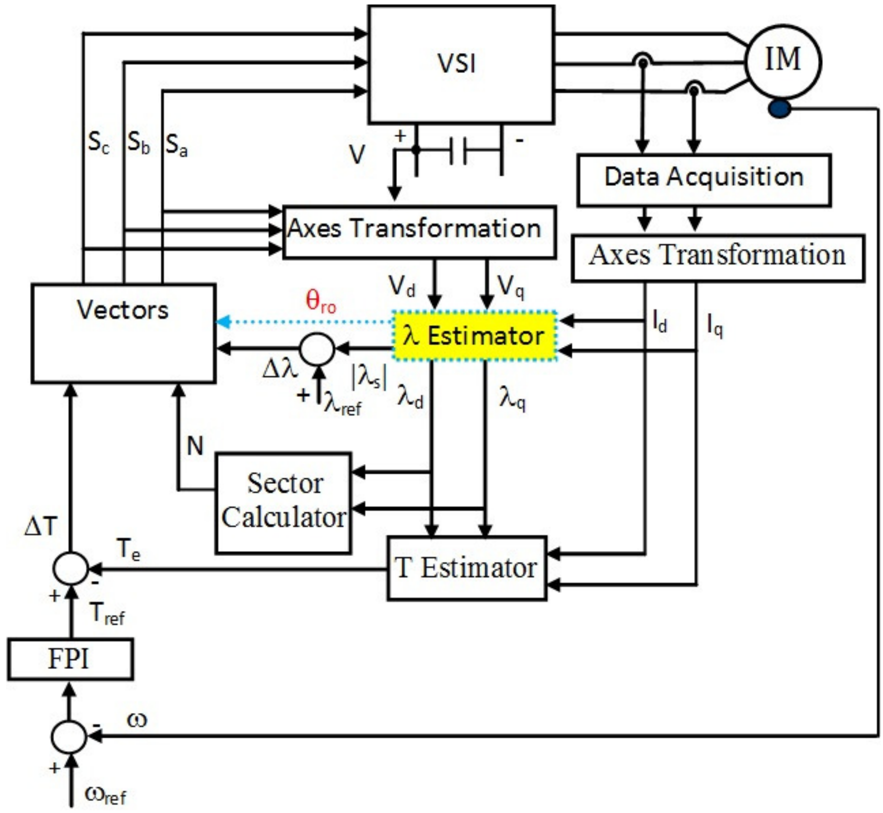

Figure 3: General block diagram of the new DTC method.

4.1. Fuzzy PID controller design

A lot of researches are done on the new PID control strategies based on intelligent algorithms especially using fuzzy logic concepts [24-30]. The proposed self-tuning fuzzy PID controller is a combination of fuzzy logic principles and the conventional PID controller. The self-tuning fuzzy PID controller utilizes the Fuzzy Interface System (FIS) to tune the parameters of K_p, K_i, and K_d according to speed error (e) and the derivative of the speed error ($\Delta e(t)$). The block diagram of speed control of Induction motor is shown in Figure 4. The structure of self-tuning fuzzy PID controller is shown in the Figure 5.

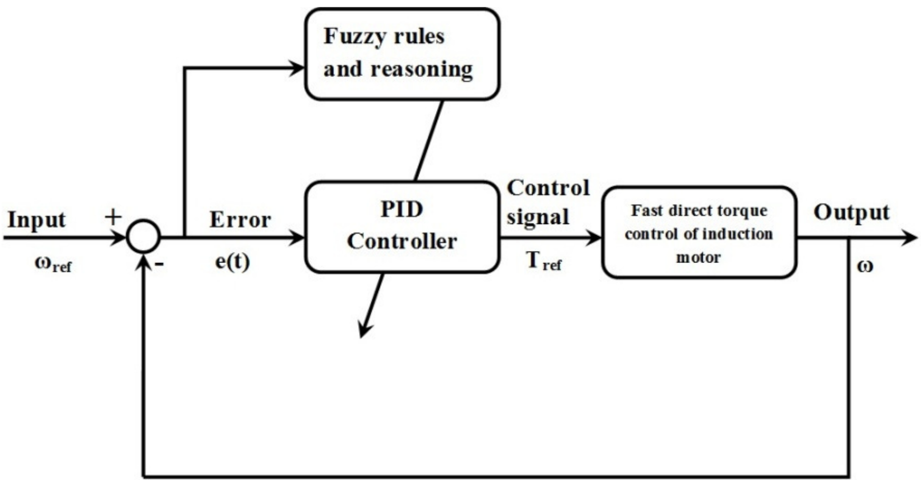

Figure 4. The block diagram of speed control of Induction motor.

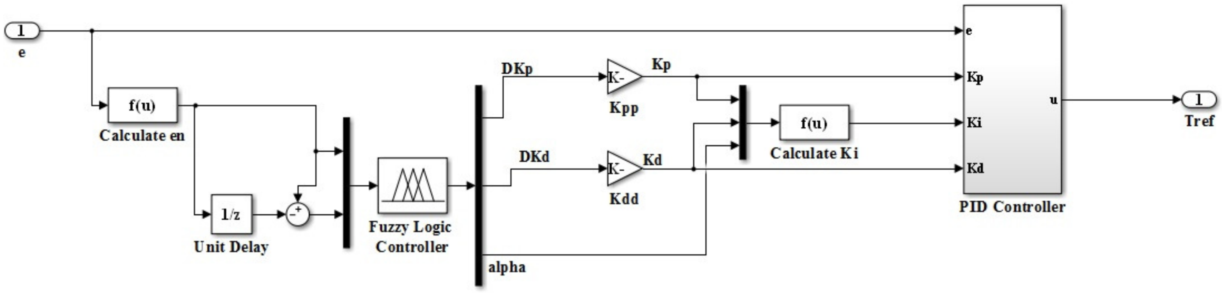

Figure 5: The structure of self-tuning fuzzy PID controller.

The approach taken here is to exploit fuzzy rules and reasoning to produce controller parameters of PID controller, where

$$u = K_p e + K_i \int edt + K_d \frac{de}{dt} \tag{13}$$

Where; u is the controller signal which is the reference torque (T_{ref}) for fast DTC of induction motor.

The PID controller parameters (K_p, K_i, K_d) are defined based on the current speed error $e(t)$ and its first difference $\Delta e(t)$, where

$$e(t) = \omega(t) - \omega_{ref}(t) \tag{14}$$

$$\Delta e(t) = e(t) - e(t-\tau) \tag{15}$$

Where; τ is the sampling time.

ω, and $\omega_{ref.}$: speed and reference speed of fast DTC of induction motor.

Fuzzification of e and Δe will be explained on section **4.1.1**. Fuzzification of controller parameters will be introduced in section **4.1.2**. Fuzzy reasoning and defuzzification will be discussed in section **4.1.3**.

4.1.1. Fuzzification of e and Δe

e and Δe are assumed to be defined in prescribed ranges [$\boldsymbol{e}_{\min}$, $\boldsymbol{e}_{\max}$] and [$\boldsymbol{\Delta e}_{\min}$, $\boldsymbol{\Delta e}_{\max}$], respectively. For appropriateness, e and Δe are normalized into the ranges between zero and one by using the following linear transformation:

$$e_n(m) = \frac{e(m) - e_{\min}}{e_{\max} - e_{\min}} \tag{16}$$

$$\Delta e_n(m) = \frac{\Delta e(m) - \Delta e_{\min}}{\Delta e_{\max} - \Delta e_{\min}} \tag{17}$$

Finer fuzzy partition with seven terms [27] is used to specify the domain of each linguistic value for actual numerical values of e and Δe. The finer fuzzy partition with seven terms specifies the linguistic values NB: negative big, NM: negative medium, NS: negative small, ZE: zero, PS: positive small, PM: positive medium, and PB: positive big. A triangular membership function is assigned to each linguistic value. Figure 6 displays the membership function for the e_n and Δe_n.

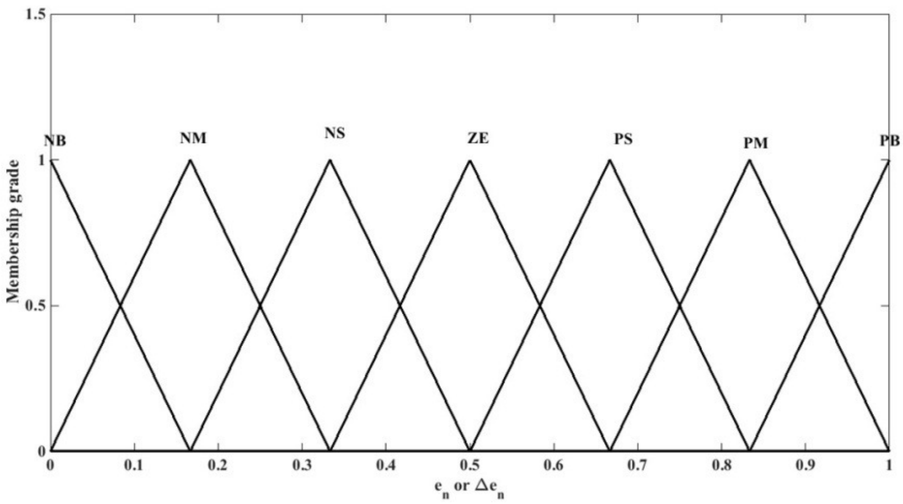

Figure 6: The membership function for e_n and Δe_n .

4.1.2. Fuzzification of the controller parameters

It is assumed that ΔK_p and ΔK_d are in fixed range $[0,1]$. ΔK_p and ΔK_d are the change in the proportional and derivative gains that adapt the proportional and derivative parameters of PID controller, as follows:

$$K_p = K_{pp} \bullet \Delta K_p \tag{18}$$

Where; K_{pp} : Multiplication factor for proportional gain and has been chosen to be 12.

$$K_d = K_{dd} \bullet \Delta K_d \tag{19}$$

Where; K_{dd} : Multiplication factor for derivative gain and has been chosen to be 20.

The linguistic values for ΔK_p and ΔK_d are assumed to be either small or big and assigned the Gaussian membership functions [27]. Figure 7 shows the membership function for the ΔK_p and ΔK_d.

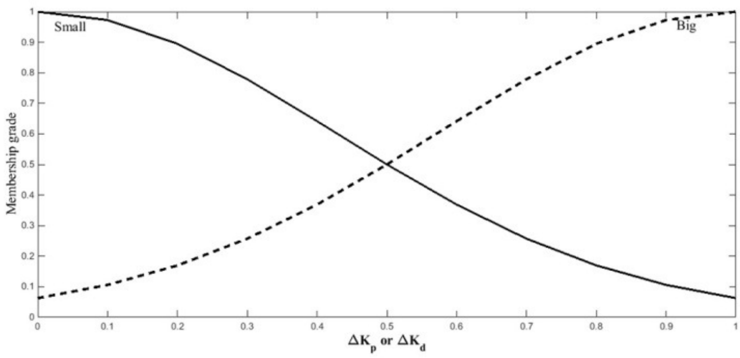

Figure 7: The membership function for ΔK_p and ΔK_d.

The integral gain is determined with reference to the proportional and derivative parameters [31], i.e.,

$$K_i = \frac{K_p^{\ 2}}{\alpha K_d} \tag{20}$$

Where ; α : integral parameter.

The linguistic values for α are supposed to be either S (small), MS (medium small), M (medium) or B (big) [27, 31]. These fuzzy sets are illustrated in singleton membership functions. Figure 8 shows the membership function for α .

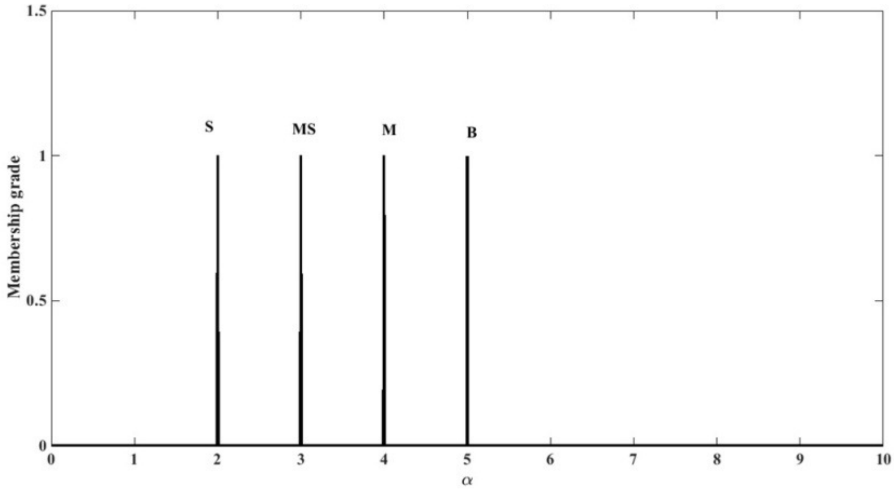

Figure 8: The membership function for α.

4.1.3. Rule base, fuzzy reasoning and defuzzification

The change of gain parameters ΔK_p and ΔK_d are decided using set of fuzzy rules having the following form:

If $\boldsymbol{e}_{\mathbf{n}}(i)$ is A_{1l} and $\boldsymbol{\Delta e}_{\mathbf{n}}(i)$ is A_{2l}, then ΔK_p is B_{1l}, ΔK_d is B_{2l}, and α is B_{3l}.

Where; $\boldsymbol{e}_{\mathbf{n}}(i)$: is the i^{th} observation for normalized error.

$\boldsymbol{\Delta e}_{\mathbf{n}}(i)$: is the i^{th} observation for normalized first difference in error.

A_{1l}: is fuzzy set for input (1) and l^{th} rule.

B_{1l} :is fuzzy set for output (1) and l^{th} rule.

l : is equal to 1,2,3,…,R and R is the number of rules.

The rule base for the normalized gain parameters are given in Tables 1, 2 and 3. These fuzzy rules are deduced according to the experience of many times for PID parameter tuning. The rules inculde the input/output relationships that specify the control strategy.

Table 1: Fuzzy tuning rules forΔK_p.

		$\boldsymbol{\Delta e}_{\mathbf{n}}(i)$						
		NB	NM	NS	ZE	PS	PM	PB
$\boldsymbol{e}_{\mathbf{n}}(i)$	NB	B	B	B	B	B	S	B
	NM	B	B	B	B	S	B	B
	NS	B	B	B	B	B	B	B
	ZE	B	B	B	B	B	B	B
	PS	B	B	S	B	B	B	B
	PM	B	B	S	B	B	B	B
	PB	B	S	B	B	B	B	B

Table 2: Fuzzy tuning rules for ΔK_d.

		$\Delta e_n(i)$						
		NB	NM	NS	ZE	PS	PM	PB
$e_n(i)$	NB	B	B	B	B	B	B	S
	NM	B	B	B	B	B	B	S
	NS	B	B	B	B	B	S	S
	ZE	S	S	S	B	S	S	S
	PS	S	S	B	B	B	B	B
	PM	S	B	B	B	B	B	B
	PB	S	B	B	B	B	B	B

Table 3: Fuzzy tuning rules for α.

		$\Delta e_n(i)$						
		NB	NM	NS	ZE	PS	PM	PB
$e_n(i)$	NB	S	S	S	S	S	S	S
	NM	MS	MS	S	S	S	MS	MS
	NS	M	MS	MS	S	MS	MS	M
	ZE	B	M	MS	MS	MS	M	B
	PS	M	MS	MS	S	MS	MS	B
	PM	MS	MS	S	S	S	MS	MS
	PB	S	S	S	S	S	S	S

5. Simulation results

The proposed DTC system, shown in Fig. 3, is simulated using Matlab with sampling time (τ= 400μsec). A FPI controller was used for the speed control loop. The motor data and parameters are given in Table 4. The FPID controller generates the reference value of the torque (T_{ref}) for the DTC system. The reference value of the stator flux equals to the flux value at the rated conditions and is given in the table 4.

Table 4 10-KW, 6 pole, 220V, 60Hz

R_s	.294Ω	L_s	.0424H
R_r	.156Ω	J	.4kgm^2
L_m	.041H	λs	.454Wb
L_r	.0417H		

For the conventional DTC, the torque and flux controllers are hysteresis controllers of bands 8% and 5%, respectively. A speed-controlled IM system is simulated with the two techniques the conventional DTC and the fast DTC. The step torque response of the fast DTC is faster than the conventional DTC as indicated in [8]. This in turn gives faster torque loop to our system and improves the speed response.

The step speed responses of the two techniques, with 574 rpm step at full load torque, are shown in Figure 9.

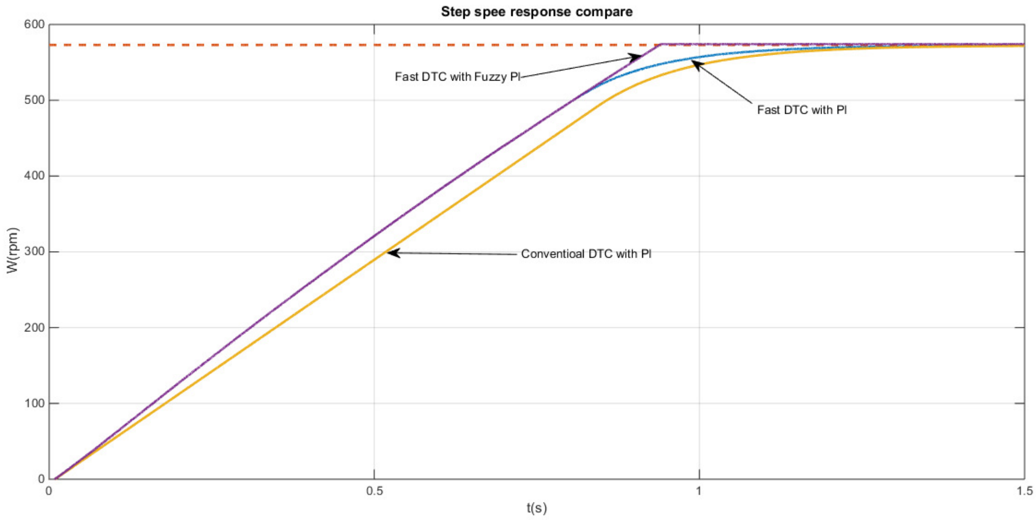

Figure 9: The step speed response.

Compared to the conventional DTC, fast DTC response is faster with PI or FPI. However, with FPI the response is the fastest and almost ideal. Also, it is noted from simulations that the speed response of the conventional PI is sensitive to the gains K_p, and K_i values that depend on the speed set value. However, the speed response with FPI is robust to the changes of the speed set value.

Figure 10 shows the full load speed response with FPI controller at different set speed values. It is clear that the system gives high performance speed response. At all set points, there were no overshoots and no steady state errors. But, the settling time differs according to the set value.

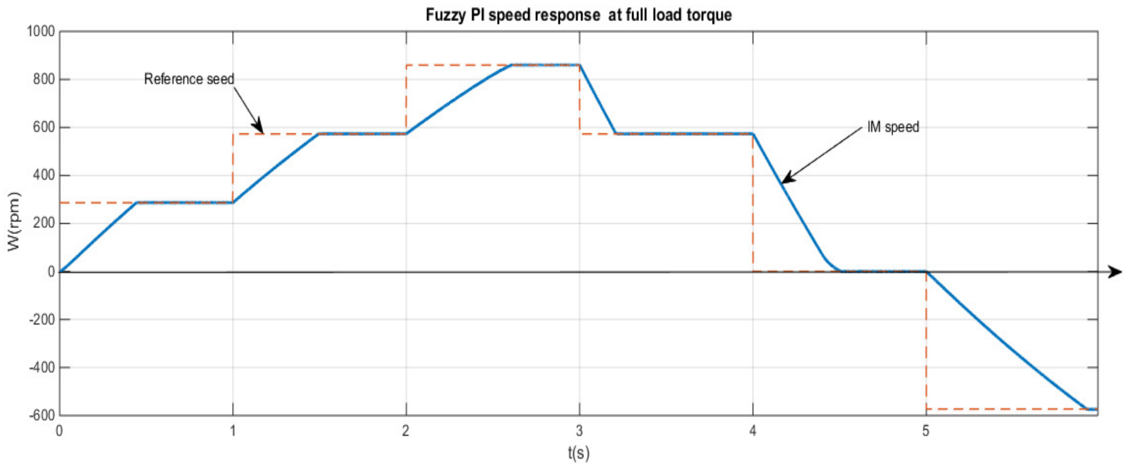

Figure 10: The speed response at full load torque and different speed set values.

Figure 11 shows the speed response at 574 rpm step speed and different set load torque values. It is clear that the speed has an ideal response and the speed is very stable to load torque T_L changes. Also, the controller output T_{ref} adjusts the torque set point to compensate for load changes.

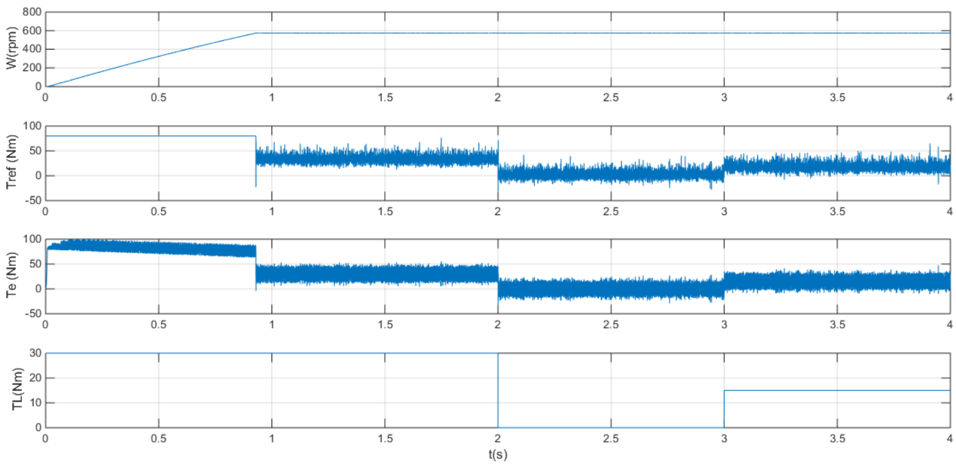

Figure 11: The speed response, T_c, and T_m at 574 rpm step speed and different set load torque values (T_L).

Obviously, the estimated IM torque (T_e) and T_{ref} perfectly track T_L. That indicates the fastness of the inner torque loop and the FPID controller. Figure 12, shows the phase current and voltage I_a and V_a at 574 rpm step speed and different set T_L values.

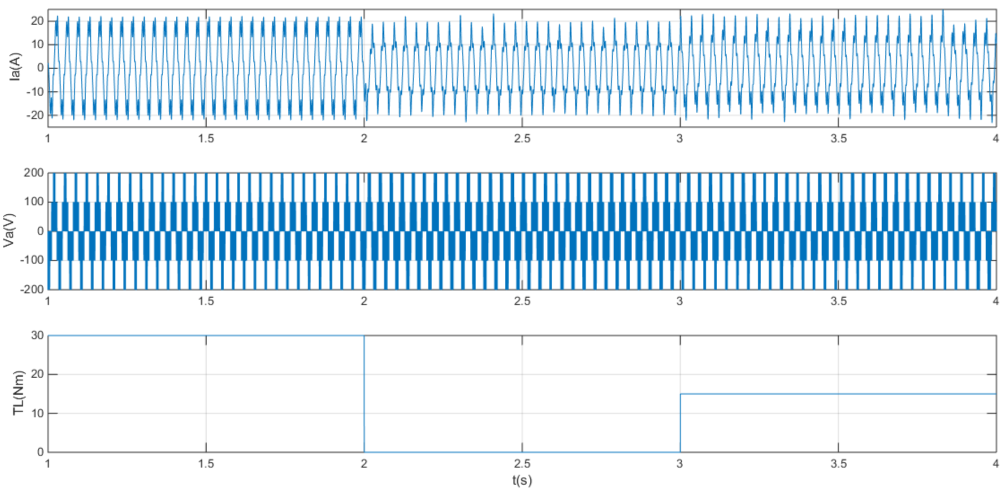

Figure 12: The phase current and voltage I_a and V_a at 574 rpm step speed and different set load torque values (T_L).

The current changes are significant; however, at no load the current is fairly high due to the magnetization of the IM magnetic circuit.

6. Conclusions

An optimization technique for fast torque response of DTC IM drives is introduced. Also, FPI controller is adapted for speed control loop. The proposed system enables fast torque, speed responses, and use of constant switching frequency. The system speed and torque responses are highly improved compared to the conventional DTC method. Theoretical work for the voltage vectors optimizations and Matlab simulations are carried out confirming the superior performance.

Simulations have been proved that the proposed system improves the performance of the DTC IM drive. Moreover the FPI enhances the fastness of the torque and seed responses compared to the PI controller.

References

[1] Lipo, T. A., Nqvotny, B.W., *Vector control and dynamics of AC drives*, Oxford University Press,1996.

[2] Buja, G.S., Kazmierkowski, M.P.: *Direct torque control of PWM inverter – fed AC motors*. IEEE Trans. Ind. Electron., 51 (4),744–757, 2004.

[3] Kazmierkowski, M.P., Franquelo, L. G., Rodriguez, J., Perez, M. A., and Leon, J. I., *High Performance Motor Drive,* IEEE Industrial Electron. Magazine, 27(1), 6–26, September 2011.

[4] Hassan, A. A., Shehata, E. G., *High Performance Direct Torque Control Schemes for an IPMSM Drive,* Electr. Power Syst. Res., 89, 171–182, August 2012.

[5] Tiitinen, P., Pohjalianen, P., Lalu, J., *The next generation motor control method DTC,* Revue ABB, 3, 19–24, 1995.

[6] TAKAHASHI, I., NOGUCHI, T., *A New Quick Response and High Efficiency Control Strategy of an Induction Motor,* IEEE Trans. Ind. Appl., 22 (5), 820–827, 1986 .

[7] Depenbrock, M., *Direct self control (DSC) of inverter fed induction machine,* IEEE Trans. Power Electron., 3 (4), 420–429, 1988.

[8] Zaid, S. A., Mahgoub, O.A., El-Metwally, K.A., *Implementation of a New Fast Direct Torque Control Algorithm for Induction Motor Drives,* IET Electr. Power Appl., 4(5), 305–313, 2010.

[9] Habetler, T.G., Profumo, F., Pastorelli, M., Tolbert, L.M., *DTC of IM Using Space Vector Modulation,* IEEE Trans. Ind. Appl., 28(5), 1045–1053, 1992.

[10] Kazmierkowski, M.P., Kasprowicz, A.B., *Improved Direct Torque And Flux Vector Control Of PWM Inverter Fed Induction Motor Drives,* IEEE Trans. Ind. Electron., 42 (4), 344–350, 1995.

[11] Lascu, C., Boldea, I., and Blaabjerg, F., *A Modified Direct Torque Control for Induction Motor Sensorless Drive,* IEEE Trans. Ind. Appl. , 36(1),122–130, Feb. 2000.

[12] Hoffmann, F. and Janecke, M., *Fast Torque Control Of An IGBT-Inverter Fed Three-Phase A.C. Drive In The Whole Speed Range Experimental Results,* In Proc. 6th Eur. Power Electron. Conf., Sevilla, Spain, 3399–3404, 1995.

[13] Carmeli, M. S., Mauri, M., *Direct Torque Control as a variable Structure control: Existence Conditions Verification and Analysis,* Electr. Power Syst. Res., 81(6), 1188–1196, June 2011.

[14] Zhang, Z., Tang, R., Bai, B., and Xie, D., *Novel Direct Torque Control Based on Space Vector Modulation With Adaptive Stator Flux Observer for Induction Motors,* IEEE Transactions on Magnetics, 46(8), pp. 3133–3136, August 2010.

[15] Shyu, K. K., Lin, J. K., Pham, V. T., Yang, M. J., AND Wang, T. W., *Global Minimum Torque Ripple Design For Direct Torque Control Of Induction Motor Drives,* IEEE Trans. Ind. Electron. , vol. 57, no. 9, pp. 3148–3156, Sep.2010.

[16] Jidin, A., Idris, N. R., Yatim, A. H. M., Sutikno, T., AND Elbuluk, M. E., *An Optimized Switching Strategy for Quick Dynamic Torque Control in DTC-Hysteresis-Based Induction Machines,* IEEE Trans. Industry Elec., 47 (5), 3391–3400, August 2011.

[17] Jidin, A., Idris, N. R., Yatim, A. H. M., Sutikno, T., AND Elbuluk, M. E., *Simple Dynamic Over modulation Strategy for Fast Torque Control in DTC of Induction Machines with Constant-Switching-Frequency Controller,* IEEE Trans. Industry App., 47 (5), 2283–2291, Jan. 2012.

[18] Patel, C., Rajeevan, P. P., Dey, A., Ramchand, R., Gopakumar, K., Kazmierkowski, M.P., *Fast Direct Torque Control of an Open-End Induction Motor Drive Using 12-Sided Polygonal Voltage Space Vectors,* IEEE Trans. Power Electronics, 27(1), 400–409, Jan. 2012.

[19] Geyer, T., Papafotiou, G., AND Morari, M., *Model Predictive Direct Torque Control—Part I: Concept, Algorithm, and Analysis,* IEEE Trans. Industry Elec., 56 (6),1894–1905, June 2009.

[20] Papafotiou, G., Kley, J., AND Papadopoulos, K. G., Bohren, P., Morari, M., *Model Predictive Direct Torque Control—Part II: Implementation and Experimental Evaluation,* IEEE Trans. Industry Elec., 56 (6), 1906–1915, June 2009.

[21] Vargas, R., Ammann , U., Hudoffsky, B., Rodriguez, J., and Wheeler, P., *Predictive torque control of an induction machine fed by a matrix converter with reactive input power control,* IEEE Trans. Power Electron. , 25(6), 1426–1438, Jun. 2010.

[22] Geyer, T., *Computationally Efficient Model Predictive Direct Torque Control,* IEEE Trans. Power Electron. ,26(10), 2804–2816, 2011.

[23] Krishnan, R., Doran, F.C., *Study Of Parameter Sensitivity In High Performance Inverter-Fed Induction Motor Drive System,* IEEE Trans. Ind. Appl., 23(4), 623–635, 1987.

[24] Kumar, R. A. and Daya, J. L. F., *a Novel indirect field oriented control of induction motor using self- tuning fuzzy PID controller,* International Journal of Systems Algorithms and Applications, 3(19), 73-77, February 2013.

[25] Kumar, R. A. and Daya, J. L. F., *a Novel self- tuning fuzzy based PID controller for speed control of induction motor drive,* International conference on control communication and computing (ICCC),62-67, 2013.

[26] Kazemian, H. B., *Comparative study of a learning fuzzy PID controller and a self-tuning controller,* ISA Transactions, 40(3), 245-253, 2001.

[27] Dorrah, H. T., El-Garhy, A. M., and El-Shimy M. E., *Design of PSO-Based Optimal Fuzzy PID Controllers for the Two-Coupled Distillation Column Process,* Proceedings of the 14th International Middle East Power Systems Conference (MEPCON'10), Cairo University, Egypt, December 19-21, 181-188, 2010.

[28] Birou, I., Maier, V., Pavel, S., and Rusu, C., *Indirect Vector Control of an Induction Motor with Fuzzy Logic Based Speed Controller,* Advances in Electrical and Computer Engineering, 10(1),116-120,2010.

[29] Kumar, V. and Joshi, R. R., *Hybrid Controller based Intelligent Speed Control of Induction Motor,* Journal of Theoretical and Applied Information Technology, 3(1), 71-75, 2003.

[30] Fini , A. M. O., Gogani, M. B., and Pourgholi, M., *Fuzzy Gain Scheduling of PID Controller Implemented on Real Time Level Control,* 4th Iranian Joint Congress on Fuzzy and Intelligent Systems (CFIS), 2015.

[31] Vahedpour, M., Noei, A. R., and Kholerdi, H. A., *Comparison Between Performance of Conventional, Fuzzy and Fractional Order PID Controllers in Practical Speed Control of Induction Motor*, 2015 2nd International Conference on Knowledge –Based Engineering and Innovation (KBEI), Iran University of Science and Technology, Tahran, Iran, November 5-6, 2015.

[32] Kandiban, R., and Arulmozhiyal R., *Design od Adaptive Fuzzy PID Controller for Speed control of BLDC Motor*, International Journal of Soft Computing and Engineering (IJSCE), 2(1), 386-391, March 2012.

[33] Xie, W., Duan, J., *The design and Simulation of Fuzzy PID Parameter Self-tuning Controller*, TELKOMNIKA Indonesian Journal of Electrical Engineering, 14(2), 293-297, 2015.

[34] Fu, L., Zhang, Z., Kong, Q., and Mao, J., *The Design of Adaptive Fuzzy PID Controller with Smith Compensator* for *Network Control Systems*, Proceeding of the 2015 IEEE International Conference on Information and Automation Lijiang, China, 3037- 3040, August 2015.

[35] He , Y., Tang, Y., Lee , D., Ahn, J., *Suspending Control Method of BLSRM Based on Adaptive Fuzzy PID Controller*, 2016 IEEE Transportation Electrification Conference and Expo, Asia - Pacific (ITEC), Busan, Korea, June 1 -4, 2016.